DOI: 10.21062/mft.2026.037 © 2026 Manufacturing Technology. All rights reserved. http://www.journalmt.com

Analysis of the Influence of Laser Welding Parameters on the Quality of the Lap Joint

Zbigniew Saternus (0000-0002-3837-1072)[1], Wiesława Piekarska (0000-0002-0185-1419)[2], Tomasz Domański (0000-0002-5375-5402)[1], Ján Vavro jr. (0009-0009-6787-9041)[3], Marcin Kubiak (0000-0002-2276-535X)[1], Pavol Čerňava (0009-0006-5455-6305)[3]
[1]Faculty of Mechanical Engineering, Czestochowa University of Technology, Dabrowskiego 69, 42-201 Czestochowa, Poland. E-mail: zbigniew.saternus@pcz.pl, tomasz.domanski@pcz.pl, marcin.kubiak@pcz.pl
[2]Faculty of Architecture, Civil Construction and Applied Arts, Academy of Silesia, Rolna 43, 40-555 Katowice, Poland wieslawa.piekarska@pcz.pl
[3]Faculty of Industrial Technologies, Alexander Dubček University of Trenčín, Ivana Krasku 491/30, 020 01 Púchov, Slovak Republic. E-mail: jan.vavro.jr @tnuni.sk, pavol.cernava@tnuni.sk

The analysis presented focuses on the relationship between laser welding parameters and the strength properties of lap joints. The objective of the research was to design a numerical model for estimating the strength properties of lap joints welded by laser beam. As part of the work, experimental tests were carried out and then numerical simulations were performed. Experimental tests were performed for a lap joint welded using two different welding depths. A joint with full and partial penetration of materials was obtained. The material used for the lap joint is two flat bars with dimensions of 100x200x2 [mm] made of X5CrNi18-10 austenitic steel. Mechanical strength measurements and macroscopic studies were performed to identify the properties of the lap joint. To identify the properties of the lap joint, mechanical strength tests and macroscopic examinations were conducted. Based on experimental studies, discrete models of the analysed lap joints were developed in the Abaqus FEM program. Simulation calculations of the laser welding process were performed. The obtained simulation results were input data for further numerical strength analysis. To validate the numerical models, the results obtained were compared with experimental data.

Keywords: Numerical modelling, Lap joint, Laser welding, Temperature field, Fusion zone, Stainless steel

1 Introduction

Among the concepts that shaped industrial progress, the application of a laser beam in welding played a particularly important role [1-4]. The development of laser techniques has provided new possibilities for making innovative welded joints [3-6]. This technology has become widely adopted in various branches of industry [3-5]. It is used to produce various types of welded joints (butt joints, spot welds, fillet joints, and lap joints) [2, 3, 5-8]. The main advantages of this welding technology are high welding speed, a narrow fusion zone, low thermal impact on the material, and the possibility of process automation and robotization [8, 9]. Welded joints do not require any finishing treatment. The advantages of laser welding have significantly contributed to the development of this technology [4, 8, 10, 11]. Laser welding techniques are continuously being improved to increase process efficiency while maintaining the quality of the obtained welded joints. Modern types of lasers with different power levels and specialized heads enable the configuration and construction of advanced welding stations [12, 13].

The laser welding process involves intricate thermomechanical interactions [7, 8, 14]. Among the parameters that significantly affect weld quality are the laser beam power and the welding speed. The correct selection of technological parameters greatly improves the quality and strength of welded joints [9]. Numerical methods can be helpful in selecting appropriate welding parameters [8, 15-18]. The latest industrial demands require fast and reliable numerical solutions across all processes in which precise prediction of material behavior is essential [19].

This paper presents a comprehensive analysis of the impact of laser welding process parameters on the quality and mechanical performance of lap-welded joints. Many industries make use of laser-welded lap joints, with the automotive industry being a key example due to its need for fast processing and high-quality welds [20-23]. Laser-welded lap joints with full joint penetration and partial joint penetration are used in industry. Partial penetration joints are applied in structural components that carry low or

medium loads. As part of this work, experimental lap joints were produced using two different welding process parameters. A lap joint with full and partial joint penetration was obtained. To evaluate the quality of the joints, strength tests and metallographic examinations were carried out [24-26]. The experimental studies provided the basis for numerical analyses.

The numerical analysis was performed using the Abaqus software based on the finite element method [8, 16]. A three-dimensional discrete finite element model of the welded joint was generated in Abaqus. The thermophysical properties of the materials were specified as temperature-dependent input data. To adapt the Abaqus program for numerical simulations of the welding process, an additional numerical subroutine, DFLUX, was implemented into the calculation procedure [8]. Based on the numerical simulations, the shape and size of the melting zones were estimated. The obtained numerical results were compared with the experiment. The next step consisted of numerically evaluating the welding process parameters that enhance the mechanical performance of the lap joint with partial joint penetration.

2 Experimental research

As part of the study aimed at evaluating the influence of laser welding parameters on joint quality, two lap joints were produced using different process settings. The welding operations were performed at the Łukasiewicz Research Network – Welding Institute in Gliwice. Joined elements in welded lap joint are two flat bars of thickness 100x200x2 mm (length x width x depth). The flat bars are made of X5CrNi18-10 stainless steel. The lap joints are welded on one side (without additional material) using welding station equipped with CO_2 laser. Shielding gas of helium (10 l/min) is fed from the face of the weld during the process. Table 1 summarizes the process parameters. The welding parameters used in the experiment resulted in lap joints exhibiting either full penetration or partial penetration. The width of the overlap was 40 mm. Welded lap joints are presented in Fig. 1.

Tab. 1 *Process parameters*

	Beam power, [W]	Efficiency	Focal length	Welding speed, [m/min]
Sample I - **Full joint penetration**	3800	0.90	270	1
Sample II - **Partial joint penetration**	3800	0.90	270	1.5

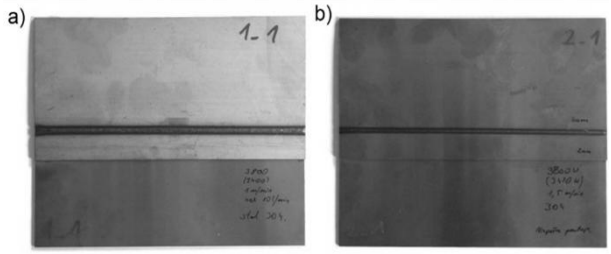


Fig. 1 *Laser welded lap joint, a) full joint penetration, b) partial joint penetration*

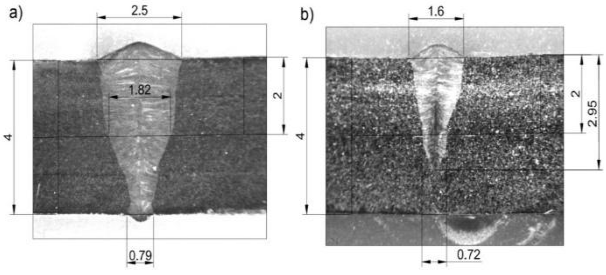


Fig. 2 *Macroscopic cross-sectional view of the weld: a) full joint penetration, b) partial joint penetration*

In the subsequent stage of the experimental study, metallographic examinations were performed to quantify the dimensions and profile of the fusion zone. The macroscopic observations of the welded joints facilitated a comparison between the experimentally obtained fusion zone geometry and the numerical simulation results. The macroscopic views are presented in Fig. 2.

Figure 2a shows a macroscopic image of a fully penetrated lap joint. The width of the weld at the point of joining the sheets is 1.82 mm, while the joint exhibiting partial melting (Fig. 2b) has a width of 0.72 mm. The penetration depth for a joint with partial joint penetration is approximately 3 mm. In order to conduct strength tests, samples were obtained from the laser welded lap joints. The tensile test specimens shown in Figure 3 were prepared with identical geometry and using the same cutting technology (water-jet cutting), which ensured repeatability of the measurement conditions. From the available welded joints, one specimen from the central region of each joint was selected for further tensile testing in order to minimize the influence of local heterogeneities.

The uniform specimen preparation and controlled testing conditions confirm the reliability of the experimental data used for the validation of the numerical model.

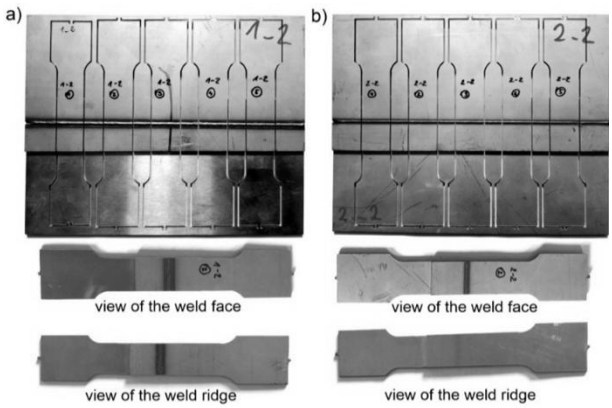


Fig. 3 *Samples for strength tests*

Tensile tests were performed on the prepared samples [8, 27, 28]. The study employed a Zwick&Roell Z100 universal testing machine with a maximum load capacity of 100 kN and a measurement accuracy of 1 N in force and 0.01 mm in displacement. Figures 4 and 5 present the obtained experimental results.

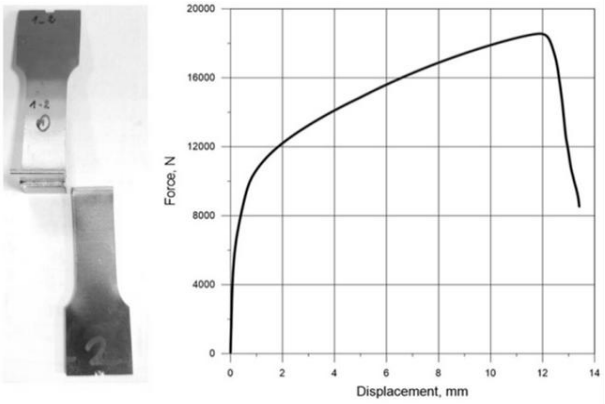


Fig. 4 *Tensile test results for a sample with full joint penetration*

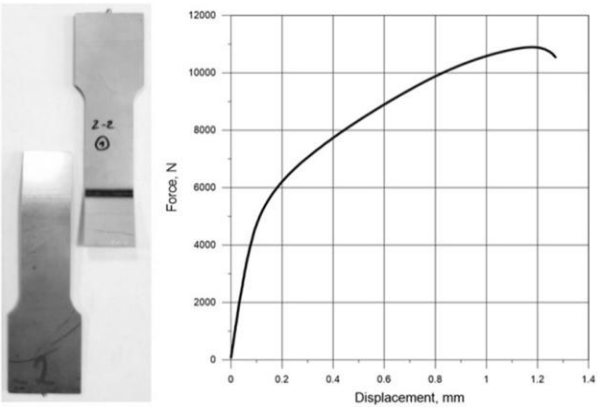


Fig. 5 *Tensile test results for a sample with partial joint penetration*

Comparing the obtained strength test results, it can be seen that the strength of the lap joint with partial joint penetration is significantly lower. There are substantial differences in both the tensile strength limit and the total elongation. The tensile strength limit R_m for the sample with full joint penetration is 251 MPa, whereas for the sample with partial penetration it is 133 MPa. Specimens with full joint penetration exhibit a gradual decrease in load after reaching the maximum force, indicating a ductile fracture with significant plastic deformation. In contrast, partially penetrated joints show an abrupt load drop, characteristic of brittle failure occurring within the joint region. In terms of elongation, the values obtained were 13.2 mm for the fully penetrated sample and 1.3 mm for the partially penetrated one. Based on the presented strength tests, it can be concluded that adjusting the welding process parameters can significantly improve the strength of lap joints with partial penetration. It can also be observed that the width of the melting zone has a considerable influence on the joint strength.

3 Mathematical and numerical modelling of laser welding

The analysis of welding processes using commercial simulation software represents a particularly demanding task, as it necessitates the formulation of suitable mathematical descriptions and the construction of a numerical model.

3.1 Mathematical model of thermal phenomena

The numerical analysis of thermal processes in Abaqus is formulated using the basic energy balance equation (1). Heat transfer is governed by Fourier's law (2). The weak formulation of the weighted residual method is defined as follows [7-9, 29, 30]:

$$\int_V \rho \dot{U}\, dV = \int_S q\, dS + \int_V r\, dV \tag{1}$$

$$f = -k\frac{\partial T}{\partial x} \tag{2}$$

Where:

V…Volume of solid material, with surface area S;

ρ…The density of the materiál;

$\dot{U}$…The material time rate of the internal energy;

q…The heat flux per unit area of the body, flowing into the body;

r…The heat supplied internally into the body per unit volume;

k…The conductivity matrix, $k=k(T)$;

f…The heat flux;

x…Position.

$$\int_V \rho \frac{\partial U}{\partial t} \delta T dV + \int_V \frac{\partial \delta T}{\partial x_\alpha} \cdot \left(\lambda \frac{\partial T}{\partial x_\alpha} \right) dV = \int_V \delta T \, q_V dV + \int_S \delta T \, q_S dS \tag{3}$$

Where:

$\lambda = \lambda(T)$…Thermal conductivity [W/mK];

$U = U(T)$…Internal energy [J/kg];

δT…Variational function;

ρ…Density [kg/m3];

qv…Volumetric heat source [W/m3];

qs…Surface heat flux [W/m2].

Equation (3) is supplemented by boundary conditions and the initial condition at $t = 0: T = T_0$, taking into account both convection and radiation:

$$T\big|_\Gamma = \widetilde{T} \quad q_{Sym} = -\lambda \frac{\partial T}{\partial n} = 0$$
$$q_S = -\lambda \frac{\partial T}{\partial n} = \alpha_k (T\big|_\Gamma - T_0) + \varepsilon\sigma(T\big|_\Gamma{}^4 - T_0^4) \tag{4}$$

Where:

q(r, 0)…Heat flux at the top surface (z = 0) within the radius r;

T_0…Ambient temperature;

α_k …Convective coefficient [W/m²K];

ε…Radiation;

σ…Stefan-Boltzman constant.

An essential component of numerical laser welding simulations is the definition of a suitable welding power distribution model. In this work, a volumetric Gaussian heat source model was implemented within the Abaqus FEA framework [30]. The model assumes a linear decay of the source energy with the penetration depth of the laser beam. In the classical Gaussian source model, the source volume is assumed to be a cylinder. For the analysed problem, the volume of the laser source was assumed to be in the shape of a truncated cone (6) [8, 9, 29].

$$Q_v(r,z) = \frac{P \cdot \eta}{\pi r_o^2 h_1} \exp\left[1 - \frac{r^2}{r_o^2}\right]\left(1 - \frac{z}{d}\right) \tag{5}$$

In which:

$$r_o = r_t - (r_t - r_b) \cdot \frac{z}{h_1} \tag{6}$$

Where:

P…Laser power [W];

r_o…Laser beam radius [m];

η…Efficiency of welding processes;

d…Material penetration depth [m];

r…Actual radius [m], r_t and r_b is beam radius, respectively for z = 0 and z = h_1;

h_1…Height of heat source penetration;

z…Actual depth of penetration [m].

3.2 Numerical model

Numerical analysis of the laser welding process for the lap joint was conducted in Abaqus FEA. A three-dimensional discrete model (3D-model) of the joint was created in Abaqus/CAE, using the geometry of the real joint as a reference. The system diagram and the adopted finite element mesh are shown in Figure 6.



Fig. 6 *Scheme of analysed domain, a) general view b) FEM view*

Figure 6b presents the finite element mesh, in which hexahedral elements of type DC3D8 were used [8, 30]. These are eight-node, three-dimensional elements commonly applied in heat-transfer analyses and welding simulations. The mesh density varies linearly, with the element size increasing proportionally to the distance from the weld line. A significant mesh refinement was introduced in the region of heat-source activity, where the highest temperature gradients occur [7-9, 16]. The minimum element size in the weld line region is 0.1 mm, and the total number of elements in the numerical model is approximately 250,000. The applied finite element mesh was selected based on the authors' experience in developing similar numerical models. Its structure represents a compromise between the accuracy of the temperature-field representation and the computational efficiency, ensuring stable and reliable simulation results. In the calculations of thermal phenomena, a simplification was introduced in the form of assuming ideal contact between the surfaces of the joined elements.

The temperature-dependent material characteristics of X5CrNi18-10 austenitic steel were implemented in the material module of Abaqus/CAE. The chemical composition of the X5CrNi18-10 steel used in the study is as follows: 0.06% C, 17–19% Cr, 11–13% Ni, and nitrogen content below 0.11%. The thermomechanical properties assumed for the numerical computations are presented in Figure 7 [8, 16].

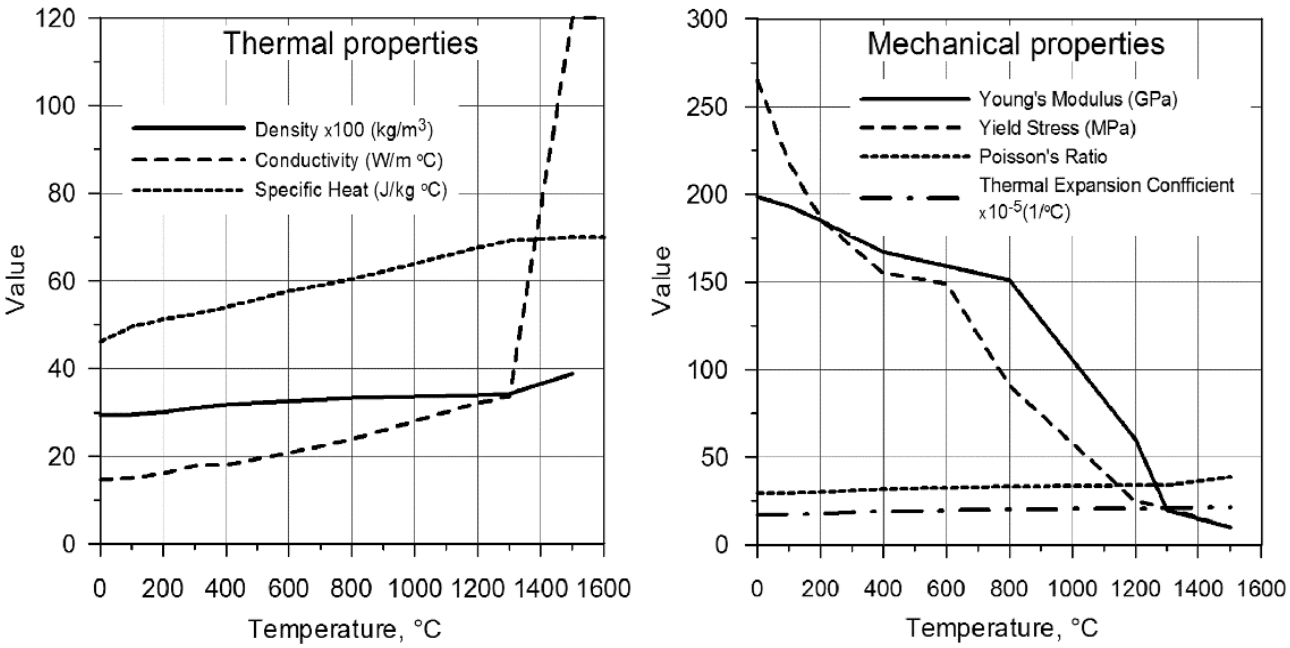


Fig. 7 *Thermomechanical material properties of welded X5CrNi18-10 stainless steel [8]*

The curves shown in Figure 7 reflect the nonlinear behavior of the material. Regarding thermophysical properties, thermal conductivity and specific heat change gradually in the lower temperature range, indicating stable heat transfer conditions. Above approximately 600°C, a distinct increase in the slope of the curve is observed, which is associated with increased heat diffusion. When analyzing the mechanical properties, it can be observed that parameters such as Young's modulus and yield strength decrease progressively with increasing temperature. The decrease is particularly rapid above 900°C, indicating a rapid loss of material stiffness near the solidus temperature. The coefficient of thermal expansion increases more rapidly at higher temperatures, consistent with the material transitioning into the solidus-liquidus range.

In the numerical simulations, the latent heat of fusion $H_L = 260 \times 10^3$ (J/kg) is applied over the solidus–liquidus temperature interval. For the X5CrNi18-10 austenitic steel, the solidus temperature was assumed: T_S = 1400 °C, liquidus T_L = 1455 °C, convective coefficient α_k = 100 W/m² K, and ambient temperature T_o = 20°C.

4 Numerical modelling results of the lap joint welding process

Numerical simulations were performed in the Abaqus/Standard solver, based on the established mathematical and numerical models. The analyses included welded joints with full and partial penetration. The heat source parameters were adopted directly from the technological parameters of the welding process. The welding process parameters adopted in the calculations are presented in Table 2.

Based on the mathematical model of the heat source (Equations 5 and 6), the beam diameter and penetration depth parameters presented in Table 2 were determined through numerical verification using the macroscopic images of the joints (Figure 2). Figure 8 presents the obtained results of numerical simulations in the cross-section for the case of full penetration 8a and partial penetration 8b. The dashed line in the figure indicates the boundaries of the liquidus temperature.

For the process parameters adopted for calculations (Table 2), good agreement of the numerical simulation results was obtained, which proves the correctness of the developed numerical models. The numerical simulation results allow for the assessment of the weld pool geometry for two sets of process parameters. In the case of the lap joint with full penetration (Figure 8a), the numerically obtained weld pool geometry closely corresponds to the actual weld geometry. The fusion zone width at the interface between the joined materials was approximately 1.75 mm, which is consistent with the macroscopic observations of the joints. For the second case (Figure 8b), corresponding to partial penetration, the numerically estimated fusion zone width was approximately 0.90 mm. The differences in temperature distributions and weld pool dimensions reflect the influence of the process parameters on heating intensity and cooling rate, which directly affect the depth of penetration and the resulting mechanical properties of the joint.

Tab. 2 *Numerical parameters of the laser welding process*

	Beam Power [W]	Efficiency	Welding speed [m/min]	Penetration deep [mm]	Beam radius [mm]
Sample I - **Full joint penetration**	3800	0.90	1	7	r_t=0.5 r_b=0.2
Sample II - **Partial joint penetration**	3800	0.90	1.5	5	r_t=0.5 r_b=0.2

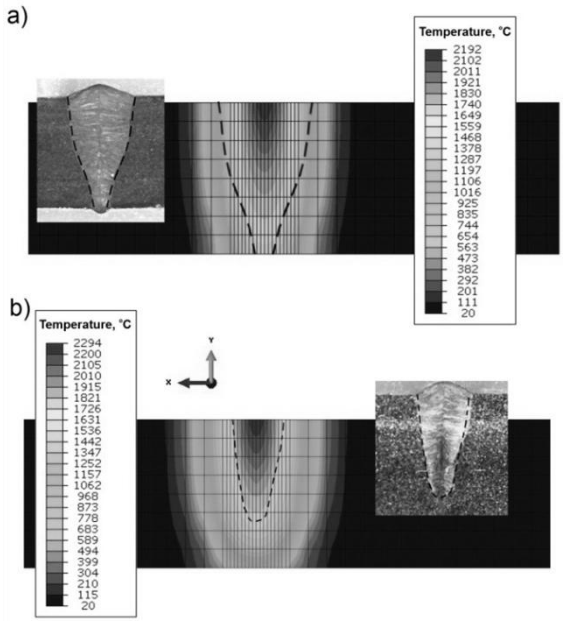


Fig. 8 *Temperature distribution in the cross section of the laser welded lap joint, a) full penetration of the joint b) partial penetration of the joint*

To evaluate the accuracy of the developed numerical model, the weld pool geometry obtained from the simulation (Fig. 8) was compared with the macroscopic cross-section views of the welded joints (Fig. 2). For the case of full joint penetration, the numerically estimated fusion zone width was approximately 1.75 mm, while the macroscopic measurement indicated 1.82 mm. This corresponds to a relative error of about 4%, confirming good agreement between the model and the experimental observations. For the case of partial joint penetration, the numerically predicted fusion width was approximately 0.90 mm, whereas the macroscopic image showed a width of 0.72 mm. This difference corresponds to a relative error of about 25%, reflecting the higher sensitivity of this configuration to process parameters and the geometric simplifications adopted in the model. Differences in temperature distributions and weld pool dimensions confirm the significant influence of the laser-beam process parameters on the shape and size of the fusion zone.

Strength tests of lap joints showed that adjusting the welding parameters for a joint with partial penetration can significantly improve its strength. To improve the strength properties of the lap joint with partial penetration, technological parameters were numerically estimated through numerical verification (Table 3). The same laser beam power as in the experiment was used, but the welding speed was adjusted. Figure 9 shows the numerically estimated temperature field for the proposed process parameters.

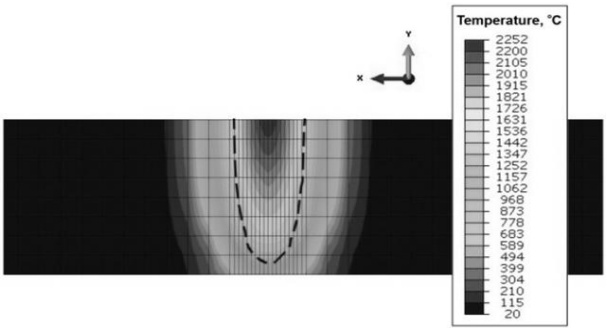


Fig. 9 *Temperature distribution in the cross section of the laser welded lap joint*

Based on the numerical calculations performed for the proposed laser beam welding parameters, the shape and size of the welded joint significantly changed. A significantly greater joint penetration depth was achieved, and the weld width was also changed. The fusion zone formed at the joining point has an approximate width of 1.4 mm, indicating that the melting was confined to a narrow region directly influenced by the laser beam.

Tab. 3 *Numerically proposed parameters for laser welding*

Beam Power [W]	**Efficiency**	**Welding speed [m/min]**	**Penetration deep [mm]**	**Beam radius [mm]**
3800	0.90	1.2	5	r_t=0.5 r_b=0.2

5 Conclusion

Changes in process parameters during laser welding of lap joints strongly affect the weld quality and its mechanical properties. Even small variations in the process parameters significantly influence the shape and size of the melting zone, which directly translates into the strength of the joint. The strength analysis of the lap joints (Figures 4 and 5) clearly shows that partial penetration leads to a considerable reduction in joint strength.

Numerical modeling of the laser welding process demonstrated very good agreement with the experimental measurements (Figure 8), which confirms the correctness of the adopted mathematical and numerical models. In the subsequent stages of the research, the verified numerical model was used to identify the parameters that improve the strength of partially penetrated joints. These results provide a quantitative basis for determining the welding conditions and constitute a foundation for further strength analyses.

The ability to predict the weld geometry and joint quality enables more efficient process planning and reduces the need for extensive experimental tests. The obtained numerical simulation results also indicate the potential of numerically estimated parameters for increasing the efficiency of industrial processes. The presented results form a basis for further research, which should focus on extending the model to include coupling thermomechanical phenomena. Expanding the parameter area and performing statistical validation on a larger set of samples would increase the robustness and applicability of the proposed methodology.

References

[1] TAYEBI, M., MOHAMMAD SOLTANI, H., RAJAEE, A. (2022). *Laser Welding*.

[2] DANIELEWSKI, H., SKRZYPCZYK, A.; HEBDA, M.; TOFIL, SZ., WITKOWSKI, G.; DŁUGOSZ, P.; NIGROVIC R. (2020) Numerical and metallurgical analysis of laser welded, sealed lap joints of S355J2 and 316L steels under different configurations. *Materials*, Vol. 13, 5819. MDPI. ISSN: 1996-1944

[3] HAOYAN, W., QIZHI, H., JIUN-SHYAN, CH., HUI-PING, W., BLAIR, E. C. (2017) Coupled thermal-mechanical-contact analysis of hot cracking in laser welded lap joints. *Journal Laser Applications.,* Vol. 29 No 2: 022412. AIP Publishing Journals. ISSN: 1938-1387

[4] XIAOHUA, W. & MINGLIANG, Z. (2025) Effect of Brass Solder Composition on Quality in Laser Welding of Solar Panel Busbar. *Manufacturing Technology Journal*, 25, 424-30. ISSN: 1213-2489

[5] NILSSON, P., ATASHIPOUR, S. R., AL-EMRANI, M. (2023). Laser-Welded Corrugated-Core Sandwich Composition—Numerical Modelling Strategy for Structural Analysis. *Journal of Composites Science*, 7(9), 349. ISSN: 2504-477X

[6] CHEN, G., HIROHATA, M., HYOMA, K. et al. (2024) Deformation and residual stress of T-shaped joints fabricated by laser-arc hybrid welding for steel bridge members. *Weld World* 68, 459–473. ISSN: 0043-2288

[7] DE, A., MAITI, S.K., WALSH, C.A., BHADESIA, K.D.H., (2003), Finite element simulation of laser spot welding. *Science Technology of Welding and Joining*, Vol. 8, No. 5, pp. 377-384. IM3. ISSN: 1362-1718

[8] DOMAŃSKI, T., PIEKARSKA, W., SATERNUS, Z., KUBIAK, M., STANO, S. (2022). Numerical Prediction of Strength of Socket Welded Pipes Taking into Account Computer Simulated Welding Stresses and Deformations. *Materials*, Vol. 15, No 9, 3243. ISSN: 1996-1944

[9] PIEKARSKA, W. (2007) Numerical analysis of thermomechanical phenomena during laser welding process. The temperature fields, phase transformation and stresses. *Wydawnictwo Politechniki Częstochowskiej*. Częstochowa. Poland

[10] CASALINO, G., DAL Maso, U., ANGELASTRO, A., CAMPANELLI, S.L. Hybrid Laser Welding: A Review. In DAAAM International Scientific Book; DAAAM International Vienna: Maria Lankowitz, Austria, 2010; Chapter 38; pp. 413–430. ISBN: 978-3-901509-74-7.

[11] KUBIAK, M., SATERNUS, Z., DOMAŃSKI, T., URBAŃCZYK, M., TALAŚKA, K., WILCZYŃSKI, D., WOJTKOWIAK, D. (2026). Modelling of Bead-on-Plate Laser Beam Melting Using Innovative Laser with a Single-Mode Core Surrounded by a Multimode Ring. *Materials*, 19(7), 1423. ISSN: 1996-1944.

[12] HAVRILLA, D., BROCKMANN, R. (2009). Third generation of disk lasers: a new benchmark for industrial solid state lasers. *Laser Technik Journal*, 6(3), 26-31. ISSN: 1614-0874

[13] PARK, J. H., MOON, H. S. (2020). Advanced automatic welding system for offshore pipeline system with seam tracking function. *Applied Sciences*, 10(1), 324. ISSN: 2076-3417

[14] KRISHMA MURTHY, K.R.; AKYEL, F.; REISGEN, U.; OLSCHOK, S. (2022) Simulation of transient heat transfer and phase transformation in laser beam welding for low alloy steel and studying its influences on the welding residual stresses. *Journal of Advanced Joining Processes*, 5, 100080. ISSN: 2666-3309

[15] SULAIMAN, S.K., ALKAHARI, M.R., JUZAILA ABD LATIF, M., HARANGAN PRASADA MANURUNG, Y. PRIAPRATAMA PRAJADHIANA, K. (2025) Thermal Analysis of Micro Plasma Wire Arc Additive Manufacturing Deposition Process. *Manufacturing Technology Journal*, 25, 396-404. ISSN: 1213-2489

[16] KORIC, S., THOMAS, B. (2007). Thermo-mechanical model of solidification processes with ABAQUS. *Proceedings of the Abaqus Users' Conference*, Paris. France. 22–24 May

[17] SAPIETOVÁ, A., DEKÝŠ, V., SAPIETA, M., PECHÁČ, P. (2014). Application of computational and design approaches to improve carrier stability. *Procedia Engineering*, 96, pp. 410-418. ISSN: 1877-7058

[18] JIMÉNEZ-XAMÁN, M., HERNÁNDEZ-HERNÁNDEZ, M., TARIQ, R., LANDA-DAMAS, S., RODRÍGUEZ-VÁZQUEZ, M., ARANDA-ARIZME, A., CRUZ-ALCANTAR, P. (2024) Numerical simulations and mathematical models in laser welding: a review based on physics and heat source models. *Frontiers in Mechanical Engineering*, vol. 10. ISSN: 2297-3079

[19] ROSLI, N.A., ALKAHARI, M.R., RAMLI, F.R., FADZLI bin Abdollah, M., IKHWAN Abdul Kudus, S., GAZALI Herawan, S. (2022). Parametric Optimisation of Micro Plasma Welding for Wire Arc Additive Manufacturing by Response Surface Methodology. *Manufacturing Technology Journal*, 22(1), 59-70. ISSN: 1213-2489

[20] HIETALA, M., JÄRVENPÄÄ, A., KESKITALO, M., JASKARI, M., MÄNTYJÄRVI, K. (2019). Tensile and fatigue properties of laser-welded ultra-high-strength stainless spring steel lap joints. *Procedia Manufacturing*, Vol. 36, pp 131-137. ISSN: 2351-9789

[21] FURUSAKO, S., MIYAZAKI, Y., & AKINIWA, Y. (2015). Tensile shear strength of laser lap joints. *Welding International*, Vol. 29, No 11, pp. 838–846. Taylor&Francis. ISSN: 0950-7116

[22] WANG, H., WANG, Y., LI, X., WANG, W., YANG, X. (2021). Influence of assembly gap size on the structure and properties of SUS301L stainless steel laser welded lap joint. *Materials*, vol. 14, 996. ISSN: 1996-1944

[23] HAN, Y., JIAXUAN, Z., LINJIE, Z. (2024), Effects of filler materials on the microstructural characteristics and mechanical properties of laser-welded lap joints of TZM alloys. *International Journal of Refractory Metals and Hard Materials*, vol. 122, 106696. *Elsevier*. ISSN: 0263-4368,

[24] BRICÍN, D., ŠPIRIT, Z., GILÍK, H., KAUFMAN, J. (2024). Effect of Laser Shock Peening on the Microstructure of P265GH Steel and X6CrNiTi18-10 Stainless Steel Dissimilar Welds. *Manufacturing Technology Journal,* 24(1), 9-14. ISSN: 1213-2489

[25] RENZHI, Zh., DAICHI, N., NINSHU, M., FENGGUI, L., TETSUO, S., TAKAYUKI T., SYUICHI Sh. (2025) Numerical modelling of laser welding pool thermal-dynamics and dissimilar materials mixing of cast iron, carbon-steel and nickel-alloy wire for weld crack prevention. *Journal of Manufacturing Processes, vol.* 156B, 398-410. ISSN 1526-6125

[26] TARABA, M., VAVRO, J., VAVRO, J. (2025). Implementation of Mechanization into the Welding Process. *Manufacturing Technology Journal,* 25(1), 120-130. ISSN: 1213-2489

[27] WAŁĘSA, K., TALAŚKA, K., WILCZYŃSKI, D. (2026). Modelling of Mechanical Properties of Thermoplastic Elastomer for Simulation of Belt Welding Process. *Acta Physica Polonica A*, 149(2), S68. ISSN: 0587-4246

[28] SHAFIQ, M. R. (2024). Effect of Laser Welding parameters on Tensile strength of different metals: Meta-analysis. *Welding Technology Review*, 96, 27–33. ISSN: 2081-2243

[29] TSIRKAS, S.A., PAPANIKOS, P., KERMANIDIS TH. (2003), Numerical simulation of the laser welding process in butt-joint specimens. In: *Journal of Materials Processing Technology*, Vol. 134, pp. 59-69. ISSN: 1873-4774

[30] DASSAULT SYSTEM (2007). Abaqus Theory Manual, Version 6.7. SIMULIA. Vélizy-Villacoublay, France